Article

2,3-Diphosphino-1,4-diphosphonium Ions

Yuen-ying Carpenter, C. Adam Dyker, Neil Burford, Michael D. Lumsden, and Andreas Decken

J. Am. Chem. Soc., **2008**, 130 (46), 15732-15741 • DOI: 10.1021/ja805911a • Publication Date (Web): 22 October 2008

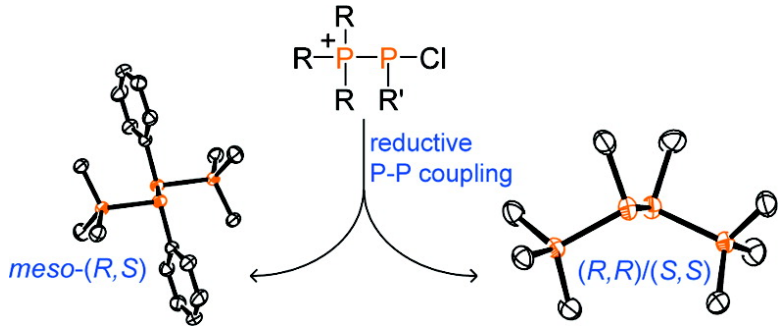

More About This Article

Additional resources and features associated with this article are available within the HTML version:

- Supporting Information
- Access to high resolution figures
- Links to articles and content related to this article
- Copyright permission to reproduce figures and/or text from this article

View the Full Text HTML

J|A|C|S
ARTICLES

Published on Web 10/22/2008

2,3-Diphosphino-1,4-diphosphonium Ions

Yuen-ying Carpenter,[†] C. Adam Dyker,[†] Neil Burford,*[,†] Michael D. Lumsden,[‡] and Andreas Decken[§]

Department of Chemistry, Dalhousie University, Halifax, NS, B3H 4J3, Canada, Atlantic Region Magnetic Resonance Center, Dalhousie University, Halifax, NS, B3H 4J3, Canada, and Department of Chemistry, University of New Brunswick, Fredericton, NB, E3A 6E2, Canada

Received July 28, 2008; E-mail: Neil.Burford@dal.ca

Abstract: Salts of the first crystallographically characterized chlorophosphinophosphonium ions have been prepared, and their reaction with Ph_3P results in reductive coupling of the chlorophosphine centers to give the first acyclic 2,3-diphosphino-1,4-diphosphonium ions, representing a key framework in the development of *catena*-phosphorus chemistry. These new salts of general formula $[R_3P\text{-}PR'\text{-}PR'\text{-}PR_3][OTf]_2$ are also obtained in a one-pot diastereoselective reaction of a dichlorophosphine, a tertiary phosphine, and trimethylsilyltrifluoromethanesulfonate. The structural and spectroscopic features of the new dications complement those of the known diphosphonium and 2-phosphino-1,3-diphosphonium dications. Quantitative ligand exchange reactions are observed when derivatives of $[Ph_3P\text{-}PR'\text{-}PR'\text{-}PPh_3][OTf]_2$ are combined with Me_3P, demonstrating the coordinative nature of the phosphine−phosphonium P−P bonds and implicating a bonding model involving the diphosphenium dication acceptor. The observed solid state structures have been interpreted in the context of computational studies.

Introduction

The strong homoatomic bond is a feature of phosphorus chemistry that has been highlighted in discussion of the diagonal relationship with carbon but has yet to be fully exploited. In this context, a diverse and extensive *catena*-phosphorus chemistry is evolving that is made possible by versatile synthetic methods for new catenated cationic frameworks.[1−8] Derivatives of phosphinophosphonium **i**,[2] diphosphonium **ii**,[9−12] 1,3-diphosphino-2-phosphonium **iii**,[5,13] and 2-phosphino-1,3-diphosphonium **iv**[14] cations represent the prototypical examples of acyclic *catena*-phosphorus cations that have been isolated and comprehensively characterized, and other P−P bonded cationic frameworks have been reported.[15] We now report the application of a new reductive coupling reaction and a ligand exchange reaction as high yield synthetic approaches to the first examples of acyclic 2,3-diphosphino-1,4-diphosphonium ions **v**.[8] In addition, counterintuitive conformational features that are observed in the solid state structures are rationalized using computational models.

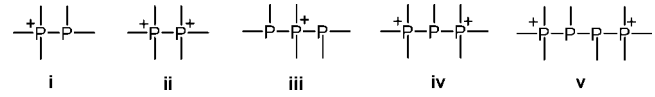

Synthetic Procedures and Characterization Data

General. Unless otherwise specified, reactions were carried out in a glovebox under an inert N_2 atmosphere. Solvents were dried on a MBraun solvent purification system and stored over 4 Å molecular sieves unless otherwise specified. MeCN was purchased anhydrous from Aldrich and used as received, Et_2O was dried by refluxing over Na/benzophenone and distilled before use, and $CHCl_3$ was degassed by three freeze−pump−thaw cycles and stored over molecular sieves for 24 h before use. Deuterated solvents were purchased from Aldrich or Cambridge Isotope Laboratories and used as received (CD_3CN, CD_3NO_2 in ampoules) or stored over molecular sieves for 24 h prior to use ($CDCl_3$). $[Ph_3P\text{-}PPhCl][OTf]$, [**1a**][OTf]; $[Ph_3P\text{-}PPh\text{-}PPh\text{-}PPh_3][OTf]_2$, [**4a**][OTf]$_2$; and $[Me_3P\text{-}PPh\text{-}PPh\text{-}PMe_3][OTf]_2$, [**4′a**][OTf]$_2$, were prepared as described in the preliminary communication.[8] $CyPCl_2$ was prepared according to literature methods.[16] Me_2PCl and $MePCl_2$ were purchased from

[†] Department of Chemistry, Dalhousie University.
[‡] Atlantic Region Magnetic Resonance Center, Dalhousie University.
[§] University of New Brunswick.

(1) Burford, N.; Cameron, T. S.; Ragogna, P. J.; Ocando-Mavarez, E.; Gee, M.; McDonald, R.; Wasylishen, R. E. *J. Am. Chem. Soc.* **2001**, *123*, 7947–7948.
(2) Burford, N.; Ragogna, P. J.; McDonald, R.; Ferguson, M. *J. Am. Chem. Soc.* **2003**, *125*, 14404–14410.
(3) Burford, N.; Ragogna, P. J. *Dalton Trans.* **2002**, 4307–4315.
(4) Burford, N.; Ragogna, P. J.; McDonald, R.; Ferguson, M. J. *Chem. Commun.* **2003**, 2066–2067.
(5) Burford, N.; Dyker, C. A.; Decken, A. *Angew. Chem., Int. Ed.* **2005**, *44*, 2364–2367.
(6) Burford, N.; Dyker, C. A.; Lumsden, M. D.; Decken, A. *Angew. Chem., Int. Ed.* **2005**, *44*, 6196–6199.
(7) Weigand, J. J.; Burford, N.; Lumsden, M. D.; Decken, A. *Angew. Chem., Int. Ed.* **2006**, *45*, 6733–6737.
(8) Preliminary Communication: (a) Dyker, C. A.; Burford, N.; Lumsden, M. D.; Decken, A. *J. Am. Chem. Soc.* **2006**, *128*, 9632–9633.
(9) Romakhin, A. S.; Palyutin, F. M.; Ignat'ev, Yu., A.; Nikitin, E. V.; Kargin, Yu., M.; Litvinov, I. A.; Naumov, V. A. *Izv. Akad. Nauk. SSSR, Ser. Khim.* **1990**, *3*, 664–669.
(10) Kilian, P.; Slawin, A. M. Z.; Woollins, J. D. *Dalton Trans.* **2006**, 2175–2183.
(11) Schomburg, D.; Bettermann, G.; Ernst, L.; Schmutzler, R. *Angew. Chem., Int. Ed. Engl.* **1985**, *24*, 975–976.
(12) Alder, R. W.; Ganter, C.; Harris, C. J.; Orpen, A. G. *Chem. Commun.* **1992**, 1170–1172.
(13) Krossing, I. *Dalton Trans.* **2002**, 500–512.
(14) Schmidpeter, A.; Lochschmidt, S.; Karaghiosoff, K.; Sheldrick, W. S. *Chem. Commun.* **1985**, 1447–1448.
(15) Dyker, C. A.; Burford, N. *Chem. Asian J.* **2008**, *3*, 28–36.
(16) Weferling, N. Z. *Z. Anorg. Allg. Chem.* **1987**, *548*, 55–62.

10.1021/ja805911a CCC: $40.75

Strem and used as received. Ph_3P, $^iPrPCl_2$, $^tBuPCl_2$, and Me_3P (1.0 M solution in toluene) were purchased from Aldrich and used as received. Ph_2PCl, $PhPCl_2$, $EtPCl_2$, and Me_3SiOTf were purchased from Aldrich and purified by vacuum distillation prior to use. $GaCl_3$ was purchased from Strem and sublimed under static vacuum prior to use.

Solution ^1H, ^{13}C, and ^{31}P NMR spectra were collected at room temperature on Bruker AC-250 (5.9 T) and Bruker Avance 500 (11.7 T) NMR spectrometers. Chemical shifts are reported in ppm relative to trace protonated solvent (^1H), to perdeuterated solvent (^{13}C), or to an external reference standard (^{31}P, 85% H_3PO_4). NMR spectra of reaction mixtures were obtained by transferring an aliquot of the bulk solution to a 5 mm NMR tube. These tubes were flame sealed, or capped and sealed with Parafilm. All reported $^{31}P\{^1H\}$ NMR parameters for second-order spin systems were derived by iterative simulation of experimental data obtained at both fields (^{31}P Larmor frequencies of 101.3 and 202.6 MHz) using gNMR, version 4.0.[17] Typically, the higher field experimental spectrum was used to find the spin system parameters, and the lower field data was subsequently used to ensure the parameters were valid at both fields. Difference calculations between simulated and experimental spectra were produced with Bruker Topspin, version 2.0,[18] using data at 202.6 MHz. The signs of the P−P coupling constants reported in Table 2 and Table 3 have been established by assigning the $^1J_{PP}$ coupling constants as negative.[19,20] Product distributions for *in situ* reaction mixtures were assessed by integration of assigned signals in the ^{31}P NMR spectra. ^{31}P NMR integrations are approximate, but are estimated to be accurate to within ±10% for identical coordination numbers or ±20% otherwise.[21] Letter designations for the phosphorus spin systems have been assigned by calculating the ratio $|\Delta\nu/J|$, where $\Delta\nu$ is the difference in ^{31}P chemical shifts in Hz, and using a value of 10 at the lower field as the threshold between a first and second order letter designation.

Infrared spectra were collected on samples prepared as nujol mulls between CsI plates using a Bruker Vector FT-IR spectrometer. Peaks are reported in wavenumbers (cm^{-1}) with ranked intensities in parentheses, where a value of one corresponds to the most intense peak in the spectrum. Melting points were obtained on samples flame-sealed in glass capillaries under dry nitrogen using an Electrothermal apparatus. Chemical analyses were performed on selected compounds by Canadian Microanalytical Services Ltd., Delta, British Columbia, Canada.

Unless otherwise stated, crystals for single crystal X-ray diffraction studies were obtained by vapor diffusion at room temperature. Samples were dissolved in a minimal amount (1−2 mL) of a polar solvent in a 5 mL vial placed within a capped 20 mL vial containing ~5 mL of a less polar solvent (solvents are indicated in the text as polar/nonpolar pairs). After deposition of crystals, the solvent was carefully removed using a pipet and the crystals were coated with Paratone oil. Single crystal X-ray diffraction data were collected using a Bruker AXS P4/SMART 1000 diffractometer. All measurements were made with graphite monochromated Mo Kα radiation. The data were reduced (SAINT)[22] and corrected for absorption (SADABS)[23] and were corrected for Lorentz and polarization effects. The structures were solved by direct methods and expanded using Fourier techniques. Full matrix least-squares refinement was carried out on F^2 data using the program SHELX97.[24] Non-hydrogen atoms were refined anisotropically. Refinement details are summarized in Table 1.

Preparation and Isolation. [Ph_3P-PPh(Cl)][$GaCl_4$], [1a][$GaCl_4$]: $PhPCl_2$ (27.1 μL, 0.20 mmol), was added to a stirred solution of Ph_3P (52 mg, 0.20 mmol) and $GaCl_3$ (39 mg, 0.22 mmol) in CH_2Cl_2 (1 mL). After 15 min, the $^{31}P\{^1H\}$ NMR spectrum of the reaction showed near quantitative formation of [**1a**][$GaCl_4$] (94%) along with $PhPCl_2-GaCl_3$ (156 ppm). Attempted isolation by addition of Et_2O yielded an oil.

[Me_3P-PPh(Cl)][OTf], [1′a][OTf]: Me_3P (1.0 M in toluene, 2 × 100.0 μL, 0.20 mmol) was added to a stirred solution of $PhPCl_2$ (27.1 μL, 0.20 mmol) and Me_3SiOTf (39.8 μL, 0.22 mmol) in CH_2Cl_2 (0.80 mL). After 1.5 h, the $^{31}P\{^1H\}$ NMR spectrum of this reaction mixture showed quantitative formation of [**1′a**][OTf].

General Procedure for [Ph_3P-PR′(Cl)][OTf], [1b−e][OTf]: $R'PCl_2$ (0.20 mmol) was added to a stirring solution of Ph_3P (52 mg, 0.20 mmol) in CH_2Cl_2 (0.5−1 mL) followed immediately by the addition of Me_3SiOTf (39.8 μL, 0.22 mmol). Attempted isolation of [**1c−e**][OTf] by addition or vapor diffusion of Et_2O yielded an oil.

[Ph_3P-PMe(Cl)][OTf], [1b][OTf]: After 1 h, the $^{31}P\{^1H\}$ NMR spectrum of the reaction showed quantitative formation of [**1b**][OTf]. Vapor diffusion of Et_2O into this solution overnight at room temperature afforded colorless needle-like crystals that were washed with Et_2O (2 × 1 mL) and dried *in vacuo*. Yield (crystalline): 63 mg (64%), mp 117−119.5 °C; FT-IR: 3063 (19), 1586 (10), 1443 (5), 1260 (1), 1189 (20), 1144 (13), 1106 (15), 1029 (7), 996 (16), 891 (18), 873 (8), 751 (6), 725 (14), 690 (4), 637 (2), 573 (11), 545 (9), 506 (3), 460 (17), 301 (12).

[Ph_3P-PEt(Cl)][OTf], [1c][OTf]: Quantitative formation of [**1c**][OTf] was observed after 10 min by $^{31}P\{^1H\}$ NMR spectroscopy.

[Ph_3P−P^{i}Pr(Cl)][OTf], [1d][OTf]: [**1d**][OTf] was observed as broad resonances (82 ppm and 16 ppm) at 298 K in the $^{31}P\{^1H\}$ NMR spectrum of the solution after 1 h, together with $^iPrPCl_2$ (*ca.* 15%). Quantitative formation of [**1d**][OTf] was observed at 213 K.

[Ph_3P-PCy(Cl)][OTf], [1e][OTf]: [**1e**][OTf] was observed as broad resonances (76 ppm and 18 ppm) at 298 K in the ^{31}P NMR spectrum of the reaction mixture after 1 h, together with $CyPCl_2$ (*ca.* 23%). Quantitative formation of [**1e**][OTf] was observed at 202 K.

[Me_3P-PCy(Cl)][OTf], [1′e][OTf]: Me_3P (1.0 M in toluene, 3 × 73.4 μL, 0.22 mmol) was added to a stirred solution of $CyPCl_2$ (41.4 mg, 0.22 mmol) in CH_2Cl_2 (1 mL) yielding a white precipitate. Upon addition of Me_3SiOTf (43.8 μL, 0.24 mmol), this solid redissolved and produced a white precipitate after 5 min of stirring. The $^{31}P\{^1H\}$ NMR spectrum of this reaction mixture after 1 h showed the presence of only [**1′e**][OTf].

[Ph_3P−P^{t}Bu(Cl)][OTf], [1f][OTf]: A solution of Ph_3P (105 mg, 0.40 mmol) in CH_2Cl_2 was added to a stirred solution of $^tBuPCl_2$ (64 mg, 0.40 mmol) in CH_2Cl_2 (total volume *ca.* 1 mL) followed immediately by the addition of Me_3SiOTf (79.6 μL, 0.44 mmol). The $^{31}P\{^1H\}$ NMR spectrum (213 K) of the reaction mixture after 2 h was interpreted as a mixture of [**1f**][OTf] and $^tBuPCl_2$ (200.0 ppm). The $^{31}P\{^1H\}$ NMR spectrum (213 K) of the reaction mixture after 48 h indicated the presence of small amounts of [Ph_3PCl][OTf] and [**5f**][OTf] ([Ph_3P−P^{t}Bu-P^{t}Bu(Cl)][OTf], AMX spin system, not simulated, approximate shifts −2 ppm (t), 24 ppm (dd), and 112 ppm (dd)).

[Ph_3P−P^{t}BuCl][$GaCl_4$], [1f][$GaCl_4$]: A mixture of Ph_3P (52 mg, 0.20 mmol), $^tBuPCl_2$ (32 mg, 0.20 mmol) and $GaCl_3$ (39 mg, 0.22 mmol) in CH_2Cl_2 (1 mL) was stirred for 1 h at room temperature, and the $^{31}P\{^1H\}$ NMR spectrum at 298 K was interpreted as a mixture of $^tBuPCl_2-GaCl_3$ (184 ppm, 98%,) and [**1f**][$GaCl_4$] (2%).

(17) Budzelaar, P. H. M. *gNMR for Windows*, 4.0; Cherwell Scientific Publishing Limited: Oxford, UK, 1997.
(18) *Topspin for Windows*, 2.0, patchlevel 5; Bruker Biospin GmbH: Germany, 2006.
(19) Finer, E. G.; Harris, R. K. *Prog. Nucl. Magn. Reson. Spectrosc.* **1971**, *6*, 61–118.
(20) Forgeron, M. A. M.; Gee, M.; Wasylishen, R. E. *J. Phys. Chem.* **2004**, *108*, 4895–4908.
(21) Huynh, K.; Rivard, E.; LeBlanc, W.; Blackstone, V.; Lough, A. J.; Manners, I. *Inorg. Chem.* **2006**, *45*, 7922–7928.
(22) *SAINT 7.23A*; Bruker AXS, Inc: Madison, Wisconsin, 2006.
(23) Sheldrick, G. M. *SADABS*; Bruker AXS, Inc.: Madison, Wisconsin, 2004.

Table 1. Crystallographic Data

(a) Crystallographic Data for Chlorophosphinophosphonium Triflate Salts

	[Ph_3P-PPh(Cl)][OTf] **[1a][OTf]**[8]	[Ph_3P-PMe(Cl)][OTf] **[1b][OTf]**
CCDC #	605574	694816
Formula	$C_{25}H_{20}ClF_3O_3P_2S$	$C_{20}H_{18}ClF_3O_3P_2S$
molecular weight (g/mol)	554.86	492.79
crystal system	monoclinic	triclinic
space group	*Pn*	$P\bar{1}$
color, habit	colorless plate	colorless plate
a /Å	10.0707(16)	8.3728(10)
b /Å	8.8891(15)	11.0797(13)
c /Å	14.166(2)	12.4662(15)
α /°	90	83.4150(10)
β /°	104.192(3)	72.798(2)
γ /°	90	85.040(2)
V /Å^3	1229.5(3)	1095.8(2)
T /K	173(1)	198(1)
Z	2	2
crystal size/mm^3	0.40 × 0.125 × 0.025	0.50 × 0.30 × 0.10
μ/mm^{-1}	0.420	0.461
$2\theta_{max}$ /°	54.98	54.98
reflections collected	8149	7617
independent reflections	4027	4767
R_{int}	0.0256	0.0177
parameters	396	358
R_1[a] ($I > 2\sigma(I)$)	0.0256	0.0347
wR_2[b] (all data)	0.0630	0.0972
GOF[c]	1.031	1.065
$\Delta\rho$ max and min /e Å^{-3}	0.309, −0.176	0.382, −0.228

(b) Crystallographic Data for Salts of 2,3-Diphosphino-1,4-diphosphonium Triflate Salts

	[Ph_3P-PPh-PPh-PPh_3][OTf]$_2$ **[4a][OTf]$_2$**[8]	[Ph_3P-PMe-PMe-PPh_3][OTf]$_2$ **[4b][OTf]$_2$**	[Ph_3P-PEt-PEt-PPh_3][OTf]$_2$ **[4c][OTf]$_2$**	[Me_3P-PPh-PPh-PMe_3][OTf]$_2$ **[4′a][OTf]$_2$**[8]	[Me_3P-PMe-PMe-PMe_3][OTf]$_2$ **[4′b][OTf]$_2$**
CCDC #	605575	694391	694390	605576	694392
Formula	$C_{10}H_{24}F_6O_6P_4S_2$	$C_{40}H_{36}F_6O_6P_4S_2$	$C_{42}H_{40}F_6O_6P_4S_2$	$C_{20}H_{28}F_6O_6P_4S_2$	$C_{10}H_{24}F_6O_6P_4S_2$
molecular weight (g/mol)	1038.82	914.69	942.74	666.42	542.29
crystal system	monoclinic	monoclinic	monoclinic	monoclinic	monoclinic
Space group	$P2_1/n$	$P2_1/c$	$C2/c$	$P2_1/c$	$P2_1/c$
color, habit	Colorless plate	colorless rod	colorless rod	colorless irregular	colorless irregular
A /Å	10.942(4)	8.761(5)	15.5968(16)	8.9520(14)	12.431(2)
B /Å	20.769(7)	27.114(17)	14.5043(16)	16.597(3)	13.520(3)
C /Å	11.462(4)	17.578(11)	19.895(2)	10.0504(16)	13.883(3)
α /°	90	90	90	90	90
β /°	113.120(6)	96.807	102.483(2)	101.328(3)	94.872(3)
γ /°	90	90	90	90	90
V /Å^3	2395.7(15)	4146(4)	4394.3(8)	1464.1(4)	2324.7(7)
T /K	173(1)	173(1)	173(1)	173(1)	198(1)
Z	2	4	4	2	4
crystal size/mm^3	0.45 × 0.275 × 0.075	0.45 × 0.10 × 0.10	0.50 × 0.20 × 0.20	0.60 × 0.40 × 0.20	0.50 × 0.25 × 0.20
μ/mm^{-1}	0.318	0.356	0.338	0.473	0.574
$2\theta_{max}$ /°	55.00	55.00	55.00	55.00	55.00
reflections collected	16121	27998	15089	9319	15518
independent reflections	5349	9274	4932	3253	5164
R_{int}	0.0239	0.0583	0.0263	0.0477	0.0380
parameters	387	525	272	228	261
R_1[a] ($I > 2\sigma(I)$)	0.0499	0.0460	0.0461	0.0479	0.0659
wR_2[b] (all data)	0.1450	0.1070	0.1282	0.1393	0.2112
GOF[c]	1.087	1.007	1.069	1.056	1.177
$\Delta\rho$ max and min /e Å^{-3}	1.913, −0.409	0.457, −0.359	0.820, −0.579	1.226, −0.466	0.806, −0.461

[a] $R_1 = \Sigma \mid |F_o| - |F_c| \mid / \Sigma |F_o|$. [b] $wR_2 = (\Sigma[w(F_o^2 - F_c^2)^2]/\Sigma[w(F_o^4)])^{1/2}$. [c] GOF = $[\Sigma w(|F_o| - |F_c|)^2/(n - p)]^{1/2}$, where n = number of reflections and p = number of parameters.

[Me_3P−P^tBu(Cl)][OTf], [1′f][OTf]: Me_3P (1.0 M in toluene, 2 × 100 μL, 0.20 mmol) was added to a stirred solution of ^{t}BuPCl$_2$ (32 mg, 0.20 mmol) in CH_2Cl_2 (0.5−1 mL) followed immediately by the addition of Me_3SiOTf (39.8 μL, 0.22 mmol) and the $^{31}P\{^1H\}$ NMR spectra of this solution showed nearly quantitative formation of [**1′f**][OTf].

[Me_3P−P^tBu(Cl)][$GaCl_4$], [1′f][$GaCl_4$]: Me_3P (1.0 M in toluene, 220 μL, 0.22 mmol) was added to a stirred solution of ^{t}BuPCl$_2$ (32 mg, 0.20 mmol) in CH_2Cl_2 (0.5 mL) followed immediately by the addition of $GaCl_3$ (79.6 μL, 0.44 mmol) in CH_2Cl_2 (0.5 mL). After 1 h, the $^{31}P\{^1H\}$ NMR spectrum showed essentially quantitative formation of [**1′f**][$GaCl_4$].

(24) Sheldrick, G. M. *SHELXL-97, Program for crystal structure determination*; University of Göttingen: Germany, 1997.

Table 2. $^{31}P\{^1H\}$ NMR Parameters for Phosphinophosphonium Triflate Salts[a]

cation	donor	acceptor	anion	spin system	$^{31}P_{B\ or\ X}$ [δ] (phosphonium)	$^{31}P_A$[δ] (phosphine)	$^1J_{PP}$ [Hz] (T)
3a	Ph_3P	PPh_2	$[OTf]^2$	—	15	−10	n/a
			$[GaCl_4]^2$	AB	13	−12	−340
3b	Me_3P	PMe_2	$[OTf]^5$	AX	18	−60	−275
3c	Cy_3P	PCy_2	$[OTf]^2$	AX	25	−21	−361
2a	$Ph_2(Cl)P$	PPh_2	$[GaCl_4]^{35}$	AX	73	0	−393
2b	$Me_2(Cl)P$	PMe_2	$[GaCl_4]^{35}$	AX	99	−33	−340
1a	Ph_3P	PPh(Cl)	$[OTf]^8$	AB	22	55	−333 (213 K)
1a	Ph_3P	PPh(Cl)	$[GaCl_4]$	AB	22	55	−338
1′a	Me_3P	PPh(Cl)	[OTf]	AB	26	46	−305
1b	Ph_3P	PMe(Cl)	[OTf]	AX	24	61	−313 (202 K)
1c	Ph_3P	PEt(Cl)	[OTf]	—	18	76	n/a (203 K)
1d	Ph_3P	$P^iPr(Cl)$	[OTf]	AX	22	72	−344 (213 K)
1e	Ph_3P	PCy(Cl)	[OTf]	AX	23	65	−343 (202 K)
1′e	Me_3P	PCy(Cl)	[OTf]	AX	23	76	−326
1f	Ph_3P	$P^tBu(Cl)$	[OTf]	AX	16	90	−390 (213 K)
1f	Ph_3P	$P^tBu(Cl)$	$[GaCl_4]$	AX	17	98	−398
1′f	Me_3P	$P^tBu(Cl)$	[OTf]	AX	23	95	−350
1′f	Me_3P	$P^tBu(Cl)$	$[GaCl_4]$	AX	20	94	−356

[a] Data are reported for spectra obtained at 298 K unless otherwise indicated.

Table 3. $^{31}P\{^1H\}$ NMR Parameters at 101.3 MHz for 2,3-Diphosphino-1,4-diphosphonium Triflate Salts[a]

$$R'_3P_B^{+}-P_A(R)-P_{A'}(R)-P_{B'}^{+}R'_3$$

		solvent	δ_A	δ_B	$^1J_{AA'}$	$^1J_{AB}=^1J_{A'B'}$	$^2J_{A'B}=^2J_{AB'}$	$^3J_{BB'}$
4a	$[Ph_3P$-PPh-PPh-$PPh_3]^8$	CH_2Cl_2	−33	24	−124	−343	69	51
	minor diastereomer	CH_2Cl_2	−42	22	*not simulated*			
4′a	$[Me_3P$-PPh-PPh-$PMe_3]^8$	MeCN	−52	25	−105	−305	66	56
	minor diastereomer	MeCN	−56	23	*not simulated*			
4b	$[Ph_3P$-PMe-PMe-$PPh_3]$	CH_2Cl_2	−71	26	−278	−282	78	62
		MeCN	−67	32	*not simulated*			
4′b	$[Me_3P$-PMe-PMe-$PMe_3]$	MeCN	−73	26	−238	−269	80	58
4c	$[Ph_3P$-PEt-PEt-$PPh_3]$	MeCN	−53.6	24.1	−276	−297	82	59
4d	$[Ph_3P-P^iPr-P^iPr-PPh_3]$	MeCN	−25.5	22.2	−318	−348	98	63
4e	$[Ph_3P$-PCy-PCy-$PPh_3]$	CH_2Cl_2	−34	20	*not simulated*			

[a] All spectra are AA′BB′ spin systems, with parameters derived by iterative fitting of experimental data at 298 K. Minor diastereomer shifts could not be simulated and thus are approximate if given. Chemical shifts (δ) are given in ppm and coupling constants (*J*) in Hz.

Formation of [Ph_3P-PPh_2][OTf], [3a][OTf], from [Ph_3P-PPh(Cl)][OTf], [1a][OTf]: Addition of Ph_2PCl (26.9 μL, 0.15 mmol) to a stirred solution of [**1a**][OTf], (83 mg, 0.15 mmol) in CH_2Cl_2 afforded partial conversion to [**3a**][OTf] and $PhPCl_2$ (162 ppm) after 30 min (5:1 ratio of **3a**:**1a**, as observed by $^{31}P\{^1H\}$ NMR spectroscopy).

[Ph_3P-PPh-PPh-PPh_3][OTf]$_2$, [4a][OTf]$_2$: [**4a**][OTf]$_2$ was prepared as described in the preliminary communication[8] for analysis by solid state NMR spectroscopy on a Bruker Avance 400 (9.4 T) spectrometer. ^{31}P CP/MAS NMR (162.0 MHz, 6.5 kHz spin rate, 4 mm rotor, ice cooled carrier gas): *Major diastereomer* $\delta = 24$ ppm, −40 ppm; *Minor diastereomer* $\delta = 19$ ppm, −31 ppm;

[Ph_3P-PMe-PMe-PPh_3][OTf]$_2$, [4b][OTf]$_2$: $MePCl_2$ (0.079 mL, 0.885 mmol) and Me_3SiOTf (0.266 mL, 1.47 mmol) were added to a solution of Ph_3P (0.35 g, 1.34 mmol) in $CHCl_3$ (9 mL) in a 50 mL 1-necked bulb with a Teflon stopper. The mixture was degassed by three freeze−pump−thaw cycles and subsequently heated to reflux within the closed system by use of an oil bath (∼ 60 °C). After 4 days, the resulting white precipitate was filtered, washed with $CHCl_3$ (1.5 mL) and dried *in vacuo*. Crystals were obtained by vapor diffusion from CH_3CN/Et_2O. Yield (powder): 0.224 g (0.245 mmol, 55%). D.p. 225−237 °C; elemental analysis calc'd (found): %C 52.52 (52.79), %H 3.97 (3.98); ^1H NMR (500.1 MHz, CD_3CN, 298 K): $\delta = 7.97$ ppm (t, $^3J_{HH} = 7.5$ Hz, 6H), 7.90 ppm (m, 12H), 7.81 ppm (m, 12H), 0.76 ppm (m, 6H); ^1H NMR (500.1 MHz, CD_3NO_2, 298 K): $\delta = 8.03$ ppm (m, 18H), 7.88 ppm (m, 12H), 0.95 ppm (m, 6H); ^{13}C NMR (125.8 MHz, DEPTQ135, CD_3NO_2, 298 K): $\delta = 136.0$ ppm (s, +), 134.0 ppm (s, +), 131.1 ppm (m, +), 117.1 ppm (m, −), 0.0 ppm (m, +); FT-IR: 1439 (10), 1262 (1), 1223 (12), 1152 (7), 1103 (10), 1030 (4), 995 (14), 879 (15), 755 (9), 721 (8), 692 (5), 637 (2), 572 (13), 543 (6), 511 (3), 306 (16).

[Me_3P-PMe-PMe-PMe_3][OTf]$_2$, [4′b][OTf]$_2$: Me_3P (0.235 mL, 1.0 M in toluene, 0.235 mmol) was added dropwise to a stirred mixture of [Ph_3P-PMe-PMe-PPh_3][OTf]$_2$, ([**4b**][OTf]$_2$, 0.106 g, 0.116 mmol) in CH_2Cl_2 (3 mL). After stirring for 30 min, the white precipitate was collected by filtration, and washed with CH_2Cl_2 (1 mL). Recrystallization over 1 day, by vapor diffusion with CD_3CN/Et_2O at −25 °C gave crystals that were washed with Et_2O (2 × 1 mL), and dried *in vacuo*, yield: 0.032 g (0.059 mmol, 51%); Mp 221−224 °C; elemental analysis calc'd (found): %C 22.15 (21.18), %H 4.46 (4.11); ^1H NMR (500.1 MHz, CD_3NO_2, 298 K): $\delta = 2.21$ ppm (m, 18H), 1.93 ppm (m, 6H); ^{13}C NMR (125.8 MHz, DEPTQ135, CD_3NO_2, 298 K): $\delta = 7.78$ ppm (m, +), −0.4 ppm (m, +); FT-IR: 1426 (14), 1260 (1), 1301 (13), 1225 (10), 1152 (5), 1029 (3), 966 (4), 901 (8), 861 (9), 809 (17), 768 (16), 758 (15), 680 (11), 636 (2), 573 (7), 517 (6).

[Ph_3P-PEt-PEt-PPh_3][OTf]$_2$, [4c][OTf]$_2$: [**1c**][OTf] (1.0 mmol) was prepared *in situ* in a 50 mL 1-necked bulb containing 5 mL $CHCl_3$. Me_3SiOTf (100.0 μL, 0.55 mmol) and Ph_3P (132 mg, 0.50 mmol, in *ca.* 2 mL $CHCl_3$) were added, and the solution was degassed by three freeze−pump−thaw cycles and sealed at reduced pressure. This solution was heated at reflux (∼55 °C) in the closed system for 48 h. The supernatant was decanted from the resulting white precipitate, which was then washed with cold CH_2Cl_2 (−40 °C, 2 × 0.5 mL) and Et_2O (2 × 1 mL). Addition of Et_2O (∼4 mL) to the supernatant gave a white precipitate, which was isolated by decantation and washed with cold CH_2Cl_2. Colorless needle-like

crystals were obtained by vapor diffusion from MeCN/Et_2O, yield (powder): 0.249 g (53% based on $EtPCl_2$), mp 201−203 °C; ^{1}H NMR (500.1 MHz, CD_3CN, 298 K): δ = 7.91 ppm (vt, 6H, H_a), 7.85 ppm (vq, 12H, H_b), 7.74 ppm (vt, 12H, H_c), 1.93 ppm (m, 3H, H_e), 0.55 ppm (m, 6H, H_f); ^{13}C NMR (125.8 MHz, DEPTQ135, CD_3CN, 298 K): δ = 136.91 ppm (s, +, $C_{a/b}$), 135.07 ppm (s, +, $C_{a/b}$), 132.06 ppm (t, +, C_c), 119.07 ppm (t, −, C_d), 14.26 ppm (t, −, C_e), 12.42 ppm (m, +, C_f); FT-IR: 1584 (15), 1439 (6), 1270 (1), 1224 (7), 1147 (4), 1101 (5), 1031 (2), 996 (11), 754 (10), 721 (12), 690 (8), 637 (3), 572 (14), 542 (9), 509 (13).

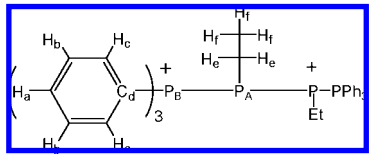

[$Ph_3P-P^iPr-P^iPr-PPh_3$][OTf]$_2$, [4d][OTf]$_2$: ^{i}PrPCl$_2$ (36.0 μL, 0.29 mmol) and Me_3SiOTf (58.1 μL, 0.32 mmol) were added to a solution of Ph_3P (77 mg, 0.29 mmol) in CH_2Cl_2 (0.60 mL). After stirring for 1 h at room temperature, this solution was transferred to a vial containing 39 mg (0.15 mmol) Ph_3P, followed by subsequent addition of Me_3SiOTf with stirring (29.1 uL, 0.16 mmol). This solution was stirred for 5 days at room temperature, resulting in the precipitation of a white powder. This solid was isolated by filtration and washed with cold CH_2Cl_2 (−40 °C, 2 × 1 mL). Dissolution of this sparingly soluble powder in MeCN and removal of the solvent *in vacuo* provided [**4d**][OTf]$_2$ (45 mg). The supernatant was analyzed by ^{31}P{^{1}H} NMR spectroscopy and showed a mixture of [**1d**][OTf], [Ph_3PCl][OTf] and a new AMX spin system (δA = −35.7 ppm, δM = 23.0 ppm, δX = 96.5 ppm, $^1J_{AM}$ = −309 Hz, $^1J_{AX}$ = −305 Hz, $^2J_{MX}$ = 59 Hz), tentatively assigned to [$Ph_3P-P^iPr-P^iPrCl$][OTf], [**5d**][OTf]. Slow evaporation of the supernatant and CH_2Cl_2 washes over 2 days yielded an additional 18 mg of [**4d**][OTf]$_2$ as a semicrystalline material. In contrast, ^{31}P{^{1}H} NMR spectra of reactions performed in more dilute solutions (<0.50 M) shown no evidence of **4d**. Instead, a mixture resembling the supernatant in more concentrated reactions was observed, with a 1:2 ratio of [Ph_3PCl][OTf] to [**5d**][OTf]. ^{1}H NMR spectra of a dilute reaction mixture (0.25 M in ^{i}PrPCl$_2$) show overlapping septets assigned as the methine resonances in **1d** (2.42 ppm) and **5d** (2.50 ppm and 2.56 ppm). The remaining ^{1}H NMR signals could not be assigned. Yield ([**4d**][OTf]$_2$): 63 mg (45%); mp 170−171.5 °C; ^{31}P{^{1}H} NMR (101.3 MHz, MeCN, 298 K): AA′BB′ spin system, δA = −25.2 ppm, δB = 22.2 ppm, $^1J_{AA'}$ = −318 Hz, $^1J_{AB}$ = $^1J_{A'B'}$ = −348 Hz, $^2J_{AB'}$ = $^2J_{A'B}$ = 98 Hz, $^3J_{BB'}$ = 63 Hz; ^{1}H NMR (500.1 MHz, CD_3NO_2, 298 K): δ = 7.87 ppm (vt, 6H, H_A), 7.68 ppm (m, 24H, $H_{B/C}$), 3.26 ppm (m, 2H, H_E), 0.93 ppm (m, 12H, H_F); ^{13}C NMR (125.8 MHz, DEPTQ135, CD_3CN, 298 K): δ = 136.60 ppm (s, +, $C_{A/B}$), 135.83 ppm (s, +, $C_{A/B}$), 131.68 ppm (t, +, C_C), 118.86 ppm (t, −, C_D), 28.11 ppm (t, +, C_E), 23.13 ppm (broad s, +, C_F); FT-IR (nujol, cm^{-1}, ranked intensities): 1439 (6), 1266 (1), 1225 (7), 1150 (4), 1098 (5), 1032 (2), 996 (11), 757 (10), 720 (13), 690 (9), 638 (3), 539 (8), 500 (12);

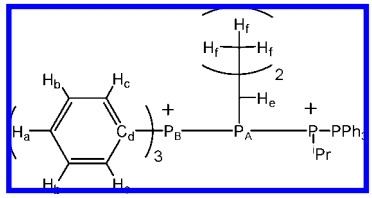

[Ph_3P-PCy-PCy-PPh_3][OTf]$_2$, [4e][OTf]$_2$: The synthesis of [**4e**][OTf]$_2$ was attempted following the procedure for [**4d**][OTf]$_2$ but with an additional equivalent of both Ph_3P and Me_3SiOTf and stirring for 40 h to maximize the yield of **4e** as observed by ^{31}P{^{1}H} NMR spectroscopy of the reaction mixture, which contains

Scheme 1. Synthesis of Chlorophosphinophosphonium Cations **1** or **1′** as Triflate or Gallate Salts

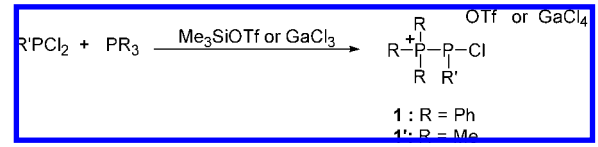

[**1e**][OTf], [**4e**][OTf]$_2$, [Ph_3PCl][OTf], and [**5e**][OTf] ([Ph_3P-PCy-PCyCl][OTf], AMX spin system, not simulated, approximate shifts −44 ppm (t), 22.5 ppm (dd), and 93 ppm (dd)).

Computational Methods. Density functional theory calculations were performed using the Gaussian 03W software package.[25] Initial geometry optimizations were performed using B3LYP/3−21G*, then further optimized to find SCF and zero-point energies with a 6−31+G(d) basis set. Initial calculations were performed on both diastereomers of [H_3P-PR′-PR′-PH_3]$^{2+}$ (R′ = Me, Ph, ^{i}Pr), where the initial C−P−P−C torsion angles ($\tau_{R'}$) were set at 0°, 60°, or 180°. Calculations on the [Me_3P-PR′-PR′-PMe_3]$^{2+}$ derivatives (**4′**) were performed using the optimized geometry results from the simplified PH_3 structure as starting geometries. Although a recent study[26] of the conformational preferences in neutral diphosphines favored the use of the B3PW91 functional for reproducing qualitative trends, experimental observations for 2,3-diphosphino-1,4-diphosphonium cations are consistent with the results provided by B3LYP.

Results and Discussion

Reaction mixtures containing a tertiary phosphine, a chlorophosphine and a chloride ion abstracting agent provide an efficient and general synthetic approach to salts of phosphinophosphonium cations **i**.[2,15] The process is considered to involve chloride ion abstraction from a chlorophosphine assisted by P−P coordination of a phosphine at the phosphorus center of the chlorophosphine, thereby stabilizing the resulting phosphenium cation. In this context, two bonding models have been employed to describe the P−P bond in phosphinophosphonium cations, one involving a covalent bond between a phosphonium and a phosphine center and the other a homoatomic coordinate bond between a phosphine donor and a phosphenium acceptor.[2] While the structural features are consistent with either bonding model, much of the established chemistry of phosphinophosphonium cations involves ligand exchange reactions, invoking a coordinate bond between the phosphorus centers.[3]

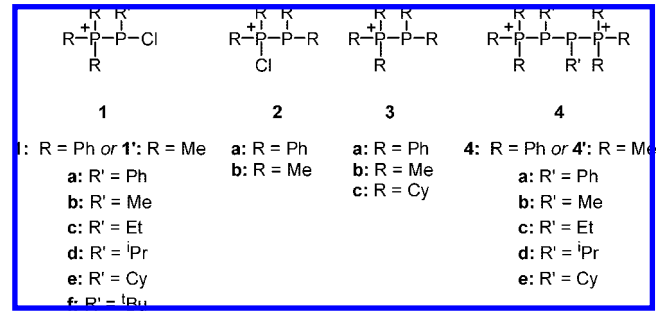

Reaction mixtures containing a tertiary phosphine, a dichlorophosphine and a chloride ion abstracting agent (Scheme 1) further generalize the quantitative synthetic approach and yield salts containing the chlorophosphinophosphonium cations **1** and **1′**, which represent isomers of the previously described phos-

(25) Frisch, M. J. et al. *Gaussian 03*, revision B.05; Gaussian, Inc.: Pittsburgh, PA, 2003.
(26) Katsyuba, S.; Schmutzler, R. *Dalton Trans.* **2008**, 1465–1470.

Scheme 2. Phosphenium (Acceptor) Exchange Reaction Yielding [**3a**][OTf] from [**1a**][OTf]

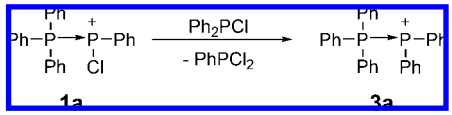

Scheme 3. Reductive Coupling Reaction of [**1**][OTf] to Give [**4**][OTf]$_2$

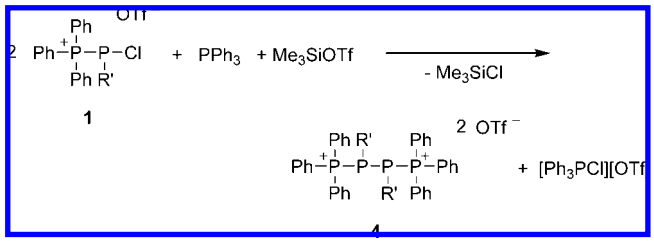

phinochlorophosphonium cations **2**[2] and variants of the organo-substituted phosphinophosphonium cations **3**.[2]

The solid state structures of [**1a**][OTf] and [**1b**][OTf] have been determined by X-ray crystallography (Table 1a) and show structural features that are consistent with those in derivatives of **2** and **3**.[2] In contrast to known derivatives of [**2**][$GaCl_4$], [**3a**][$GaCl_4$], and [**3b-c**][OTf], which exhibit two doublets at room temperature in the $^{31}P\{^1H\}$ NMR spectra (Table 2), the P−P coupling is unresolved for [**1**][OTf]; indeed, the $^{31}P\{^1H\}$ NMR spectra of [**1a-c**][OTf] exhibit two sharp singlets. This implicates increased lability of the P−P bond, and in this context, we have observed by $^{31}P\{^1H\}$ NMR spectroscopy phosphenium exchange behavior for derivatives of **1**. Solutions containing equimolar amounts of [**1a**][OTf] and Ph_2PCl give [**3a**][OTf] and $PhPCl_2$ (Scheme 2) indicating that $[PPh_2]^+$ exhibits a greater Lewis acidity toward Ph_3P than $[PPhCl]^+$, presumably due to π-interaction of nonbonding pairs on chlorine with phosphorus in $[PPhCl]^+$. In this context, diaminophosphenium cations have been shown to form Cl-bridged adducts rather than the phosphinophosphonium framework.[27] Assuming that cation **1a** dissociates in solution, we envisage exchange of chloride ion between Ph_2PCl and $[PPhCl]^+$ via $[Ph_2P\cdots Cl\cdots PPhCl]^+$ to give $PhPCl_2$ and enabling formation of the pentaphenylphosphinophosphonium cation **3a**.

The $^{31}P\{^1H\}$ NMR spectra of solutions containing [**1d**][OTf] or [**1e**][OTf] at room temperature show significant broadening of the upfield signal as well as the presence of unreacted dichlorophosphine implicating the establishment of a dissociation equilibrium. Presumably, the enhanced steric bulk at the acceptor phosphenium site favors the dissociation of the P−P bond. In addition, reaction mixtures of Ph_3P and $^tBuPCl_2$ with Me_3SiOTf or $GaCl_3$ give $^{31}P\{^1H\}$ NMR spectra at 213 K showing only 64% formation of **1f**. Nevertheless, the stronger donor Me_3P enables the quantitative formation of [**1′f**][OTf]. Unlike [**1a**−**e**][OTf], for which P−P coupling is not resolved in $^{31}P\{^1H\}$ NMR spectra at room temperature, the $^{31}P\{^1H\}$ NMR spectrum of the reaction mixture containing [**1′f**][OTf] showed doublets for both phosphorus centers ($^1J_{PP} = -350$ Hz), indicative of a stronger P−P interaction.

As illustrated in Scheme 3, addition of Ph_3P and Me_3SiOTf to derivatives of [**1a**−**d**][OTf] result in the formation of the corresponding 2,3-diphosphino-1,4-diphosphonium salts [**4a-d**][OTf]$_2$. The $^{31}P\{^1H\}$ NMR spectra of these reaction mixtures

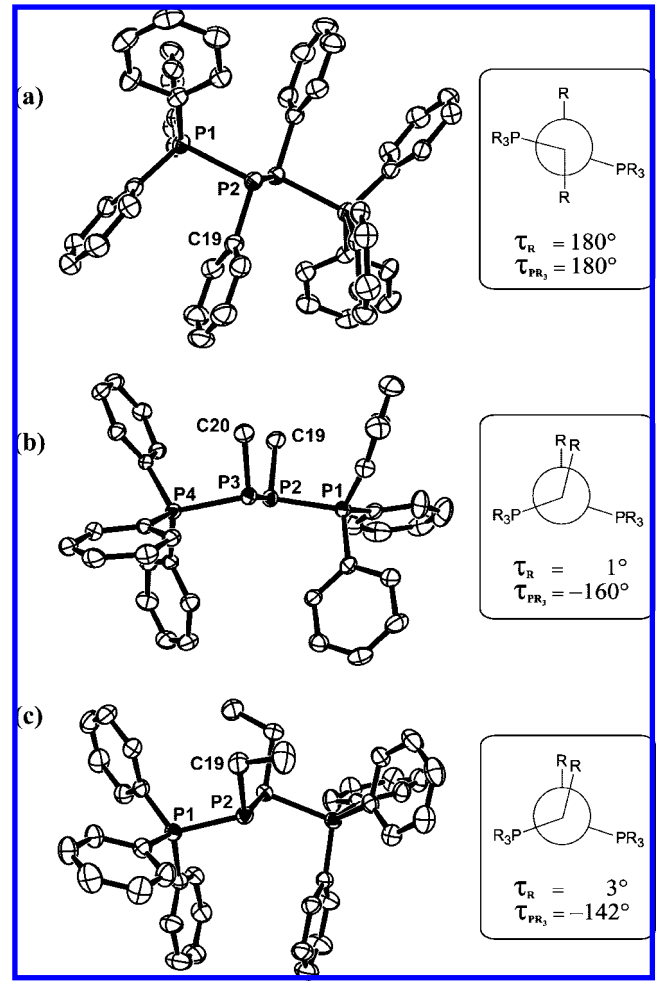

Figure 1. ORTEP representations of the solid state structure of (a) the centrosymmetric *meso*-dication in [**4a**][OTf]$_2$ and the (*S*,*S*)-enantiomer of the dication in (b) [**4b**][OTf]$_2$ and (c) [**4c**][OTf]$_2$. Thermal ellipsoids are shown at the 50% probability level and hydrogen atoms omitted for clarity. $\tau_{R'}$ indicates the C−P−P−C torsion angle between the central substituents, while τ_{PR3} indicates the P−P−P−P torsion angle of the phosphorus backbone.

show AA′BB′ spin systems (Figure 3, Table 3) assigned to **4** and a singlet corresponding to $[Ph_3PCl][OTf]$[28] ($\delta = 66$ ppm).

The AA′BB′ spin system is not observed for mixtures of [**1a**−**d**][OTf] with Ph_3P in the absence of Me_3SiOTf, suggesting that the formation of $[Ph_3PCl][OTf]$ is a key thermodynamic driving force in the P−P coupling process, rather than formation of Ph_3PCl_2. Mixtures of Ph_3P, $GaCl_3$ and [**1a**][$GaCl_4$] likewise show no evidence of reaction. Furthermore, reactions of [**1a**][OTf] with comparatively strong reducing agents such as Na or Mg give complex mixtures containing *cyclo*-Ph_5P_5[29,30] as the only product identifiable by $^{31}P\{^1H\}$ NMR spectroscopy. The $^{31}P\{^1H\}$ NMR spectra of reaction mixtures containing weaker reducing agents, such as Zn, $SnCl_2$, or cyclohexene, showed the presence of **4** together with a number of unidentified phosphorus containing products. Formation of derivatives of **4** contrast the previously reported reaction of $PhPCl_2$, Ph_3P and

(27) Burck, S.; Gudat, D. *Inorg. Chem.* **2008**, *47*, 315–321.

(28) Schmidpeter, A.; Lochschmidt, S. *Inorg. Synth.* **1990**, *27*, 253–258.
(29) Hoffman, P. R.; Caulton, K. G. *Inorg. Chem.* **1975**, *14*, 1997–1999.
(30) Smith, L. R.; Mills, J. L. *J. Chem. Soc., Chem. Commun.* **1974**, 808–809.

Scheme 4. Proposed Mechanism for the Reductive Coupling of [**1**][OTf] to [**4**][OTf]$_2$[a]

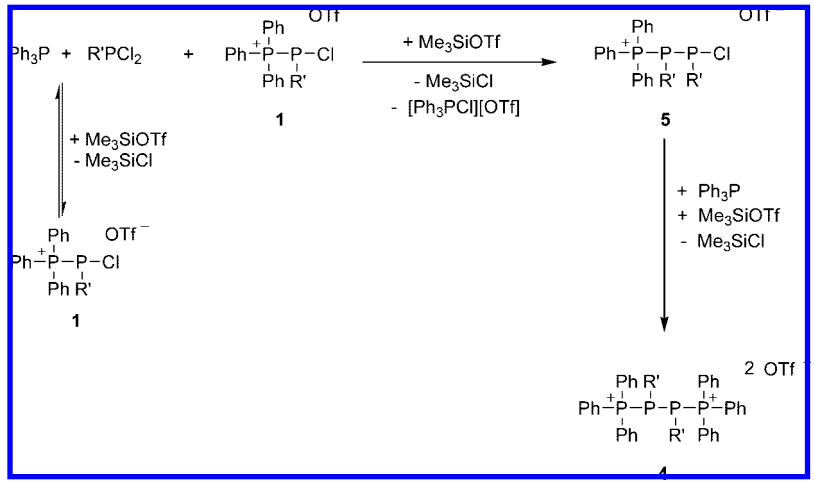

[a] Intermediate [**5d**−**f**][OTf]$_2$ has been observed by $^{31}P\{^1H\}$ NMR spectroscopy for sterically encumbered derivatives (R′ = ^{i}Pr, Cy, ^{t}Bu).

$AlCl_3$ to give [Ph_3P-PPh-PPh_3][$AlCl_4$]$_2$ (**iv**),[14] however, the formation of [**4a**][$AlCl_4$]$_2$ and its solid state structure has been described.[31]

The $^{31}P\{^1H\}$ NMR spectra of solutions containing Ph_3P, Me_3SiOTf and [**1e**][OTf] (prepared *in situ*) show partial formation of [**4e**][OTf]$_2$ after 2 days, while solutions of Ph_3P, Me_3SiOTf and [**1f**][OTf] show no evidence of [**4f**][OTf]$_2$. These observations are indicative of steric restrictions at the phosphenium site. Both of these solutions exhibit an AMX spin system, which we tentatively assign to [Ph_3P_M-P_AR'-$P_XR'Cl$][OTf], [**5**][OTf]. A similar pattern is observed as a component in solutions of Ph_3P and Me_3SiOTf with [**1d**][OTf]. In contrast to the analogue of **5** proposed by Dillon and co-workers,[32] the terminal P_X signal in this new AMX spin system (e.g., [**5d**][OTf]: $\delta A = -35.7$ ppm, $\delta M = 23.0$ ppm, $\delta X = 96.5$ ppm, $^1J_{AM} = -309$ Hz, $^1J_{AX} = -305$ Hz, $^2J_{MX} = 59$ Hz) is shifted significantly downfield relative to the P_M terminus ($\Delta\delta \geq 70$ ppm). Nonetheless, while smaller magnitude $^1J_{PP}$ coupling constants (<300 Hz) are typically observed between P(III)−P(III) spin pairs, the introduction of an electronegative substituent such as chlorine is expected to increase the magnitude of $^1J_{AX}$, justifying the similar $^1J_{AX}$ and $^1J_{AM}$ in **5**. Finally, ^1H NMR spectra of reaction mixtures containing both [**1d**][OTf] and [**5d**][OTf] indicate that the isopropyl methine ^1H signals in **5d** are 0.08−0.14 ppm downfield of the corresponding resonances in **1d**, a difference that is too small to correspond to an additonal β-Cl or positive charge adjacent to the terminal isopropyl group.[33] As shown in Scheme 4, dissociation of [**1**][OTf] is proposed to give R′PCl_2, which is subsequently reductively coupled to another molecule of [**1**][OTf] to give [**5**][OTf]. In the case of [**5d**][OTf], slow evaporation of the solvent over two days allows for the complete conversion of this mixture to [**4d**][OTf]$_2$ and [Ph_3PCl][OTf], supporting the proposal that **5** is an intermediate en route to **4**.

Selected structural parameters from the solid state structures of the dications in the triflate salts of **4a-c** (Figure 1) are presented in Table 4, where $\tau_{R'}$ indicates the C−P−P−C torsion angle between the central substituents and τ_{PR3} indicates the P−P−P−P torsion angle of the phosphorus backbone. Crystals of [**4a**][OTf]$_2$ contain the *R*,*S meso*-isomer of the dication, which is centrosymmetric with central torsion angles (τ_{PR3} and $\tau_{R'}$) of 180°. The solid state ^{31}P CP/MAS NMR spectrum for a bulk sample of crystalline [**4a**][OTf]$_2$ reveals four distinct doublet-like signals (two of lower intensity) that are also present (as more resolved AA′BB′ spin systems) in ^{31}P NMR solution spectra for redissolved crystalline samples and reaction mixtures. We conclude that the crystallographically characterized *R*,*S meso* isomer as well as the (*R*,*R*)/(*S*,*S*) diastereomeric pair are all

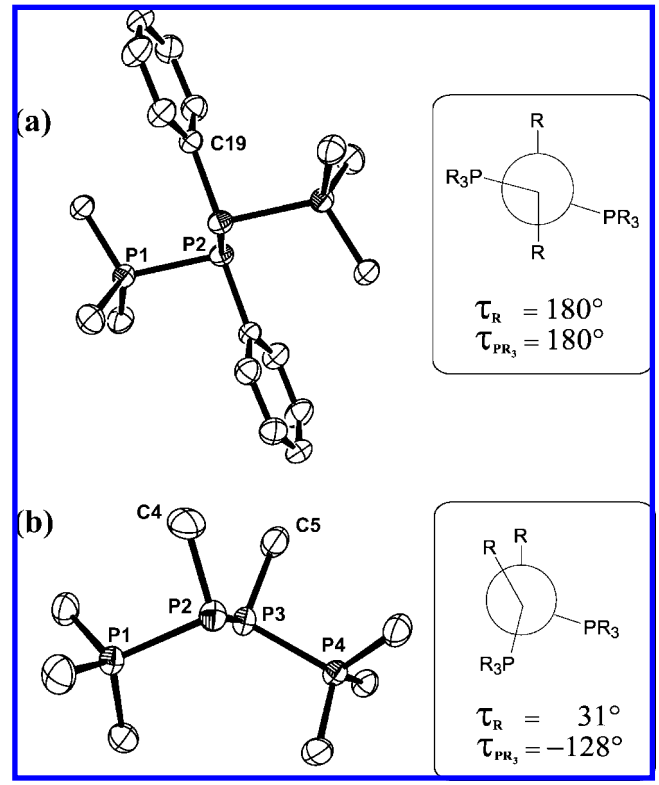

Figure 2. ORTEP representations of the solid state structure of (a) the centrosymmetric *meso*-dication in [**4′a**][OTf]$_2$ and (b) the (*S*,*S*)-enantiomer of the dication in [**4′b**][OTf]$_2$. Thermal ellipsoids are shown at the 50% probability level and hydrogen atoms omitted for clarity. $\tau_{R'}$ indicates the C−P−P−C torsion angle between the central substituents, while τ_{PR3} indicates the P−P−P−P torsion angle of the phosphorus backbone.

(31) Karaghiosoff, K. Ph.D. Thesis, Ludwig-Maximilians-Universität, Munich, Germany, 1986.
(32) Boyall, A. J.; Dillon, K. B.; Howard, J. A. K.; Monks, P. K.; Thompson, A. L. *Dalton Trans.* **2007**, 1374–1376.
(33) Beauchamp, P. S.; Marquez, R. *J. Chem. Educ.* **1997**, *74*, 1483–1485.

Table 4. Selected Solid State Structural Parameters of 2,3-Diphosphino-1,4-diphosphonium Triflate Salts

		P−P (Å)[a]	$C_{R'}$−P−P (°)[a]	$\tau_{R'}$ (°)	τ_{PR3}(°)
4a	[Ph_3P-PPh-PPh-PPh_3][8]	2.258(1) [mid] 2.221(1)	101.65(8)	180	180
4′a	[Me_3P-PPh-PPh-PMe_3][8]	2.2041(9) [mid] 2.2318(12)	101.02(8)	180	180
4b	[Ph_3P-PMe-PMe-PPh_3]	2.2061(13) [mid] 2.2284(12) 2.2125(13)	109.3(1) 107.9(1)	0.95(14)	−159.98(4)
4′b	[Me_3P-PMe-PMe-PMe_3]	2.192(2) [mid] 2.243(2) 2.191(2)	101.1(2) 102.8(2)	31.25(11)	−126.72(3)
4c	[Ph_3P-PEt-PEt-PPh_3]	2.2048(8) [mid] 2.2153(11)	109.52(9)	3.49(13)	−142.35(3)

[a] [mid] indicates the central P−P bond, while the indicated C_R'−P−P values describe the angle subtended by the central substituent (Me, Et, Ph) and this bond. $\tau_{R'}$ indicates the C−P−P−C torsion angle between the central substituents, while τ_{PR3} indicates the P−P−P−P torsion angle of the phosphorus backbone.

Scheme 5. Phosphine Exchange Reactions on Phosphinophosphonium and 2,3-Diphosphino-1,4-diphosphonium Cations

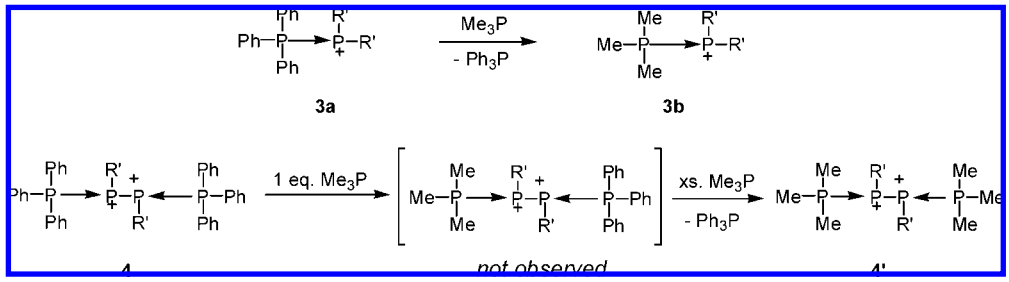

present in the bulk solid sample and in solution. The $^{31}P\{^1H\}$ NMR spectrum for the major isomer (δ = 24 and −33 ppm) has been simulated; however, the downfield signal for the minor constituent (δ = 22 and −42 ppm) was not sufficiently resolved to allow for an accurate determination of coupling constants. Integration of the ^1H NMR spectrum reveals a 62% diastereomeric excess. Although the favored diastereomer in solution could not be definitively identified, the computational results described below indicate that the *R,S meso*-isomer is thermodynamically favored in the gas phase.

Crystals of [**4b**][OTf]$_2$ contain a racemic mixture of the (*R,R*)/(*S,S*) enantiomeric pair. As shown in Figure 1, the cation adopts an essentially eclipsed conformation of the methyl substituents with a central C−P−P−C torsion angle ($\tau_{R'}$) of 0.95(14)°. Unlike [**4a**][OTf], NMR analysis of either the redissolved crystals or the reaction mixtures showed only one diastereomer, indicating that the (*R,R*)/(*S,S*) racemic mixture of [**4b**][OTf]$_2$ is formed exclusively in the reductive coupling of the racemic [**1b**][OTf]. Likewise, crystals of [**4c**][OTf]$_2$ contain an (*R,R*)/(*S,S*) racemic mixture of configurational isomers of the cation (Figure 1, Table 4), which adopt an eclipsed conformation of the ethyl substituents [$\tau_{R'}$ = 3.49(13)°] in spite of their slightly greater steric presence. Correspondingly, both **4b** and **4c** adopt larger central $C_{R'}$−P−P angles [107.9(1)−109.52(9)°] relative to **4a** [101.65(8)°] in order to minimize steric congestion.

Reaction of [**4a**][OTf]$_2$ or [**4b**][OTf]$_2$ with excess Me_3P results in quantitative formation of the corresponding derivatives of **4′**[OTf]$_2$ (Scheme 5), as indicated by the new AA′BB′ spin system in each of the $^{31}P\{^1H\}$ NMR spectra of the reaction mixtures. The reactions are best described as exchange of both terminal Ph_3P ligands for the more basic Me_3P ligands, consistent with the established ligand exchange reactivity of phosphinophosphonium cations (**2** and **3**).[2,3] Addition of only 1 equiv of Me_3P to a solution of [**4a**][OTf]$_2$ affords a 1:1 mixture of the starting dication in [**4a**][OTf]$_2$ and [**4′a**][OTf]$_2$, with no evidence for the presence of the monosubstituted product. In this context, the transformation of derivatives of [**4**][OTf]$_2$ into derivatives of [**4′**][OTf]$_2$ is conveniently understood in terms of two ligand exchange processes in which the dicationic framework of **4** (or **4′**) can be described as a bisphosphine complex of a diphosphenium ion (Scheme 5).

As observed for solutions of [**4a**][OTf]$_2$, $^{31}P\{^1H\}$ NMR spectra of [**4′a**][OTf]$_2$ show the presence of *R,S* and (*R,R*)/(*S,S*) diastereomeric pair as an unequal mixture (d.e. = 72% by ^1H NMR integration). Again, the favored diasteromer in solution could not be definitively identified, but the isolated crystalline sample contained only the centrosymmetric *R,S meso*-isomer (Figure 2). In contrast, only one diastereomer of [**4′b**][OTf]$_2$ is evident in solution, and the solid state structure (Figure 2, Table 4) contains the racemic (*R,R*)/(*S,S*) mixture in a *gauche* conformation. The smaller steric presence of the Me_3P termini in **4′b** allows for a smaller P−P−P−P torsion angle [τ_{PR3} = −126.72(3)°] compared to that in **4b** [τ_{PR3} = −159.98(4)°], thereby permitting a corresponding decrease in the proximity of the central methyl substituents [$\tau_{R'}$ = 31.35(11)°]. Consistent with the lower steric strain in **4′b**, the central $C_{R'}$−P-P angles [max. 102.8(2)] in **4′b** are smaller than those in **4b** [min. 107.9(1)°].

The second-order AA′BB′ spin systems observed in solution phase $^{31}P\{^1H\}$ NMR spectra for all derivatives of **4** are characteristic and the patterns have been simulated for most derivatives by iterative fitting with the chemical shift and coupling constant parameters listed in Table 3. An exemplar comparison of the simulated and experimental pattern is shown for [**4b**][OTf]$_2$ in Figure 3. Chemical shift parameters for the terminal phosphonium centers (δ_B) occur in a typical narrow range (20−32 ppm), while the phosphine centers (δ_A) exhibit more varied shifts ($\Delta\delta$ > 40 ppm). This is consistent with the dependence of the chemical shielding on the geometry of the phosphorus center,[34] as the tetracoordinate phosphonium centers

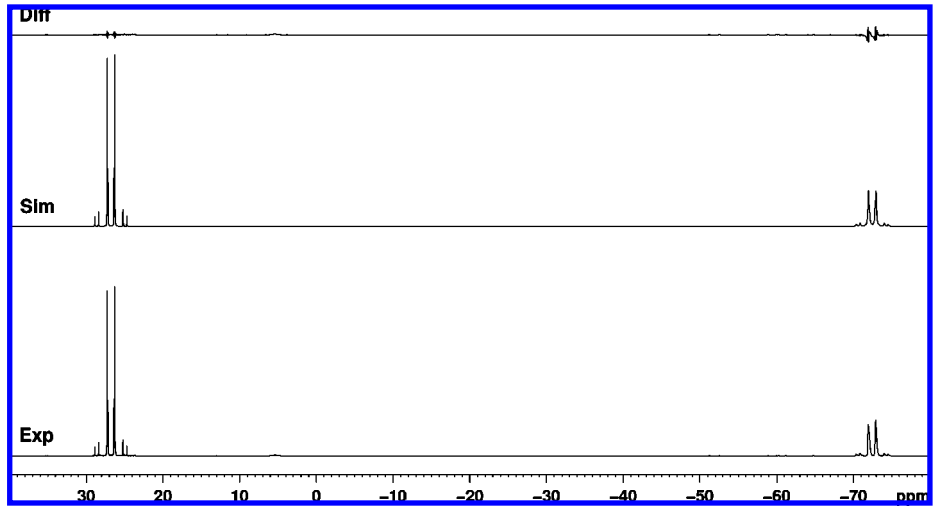

Figure 3. Comparison of simulated and experimental $^{31}P\{^{1}H\}$ NMR spectra of [**4b**][OTf]$_2$. The signal at 5.6 ppm corresponds to an impurity in the sample. Additional comparison spectra for derivatives **4′b**, **4c**, and **4d** can be found in the Supporting Information.

Table 5. Calculated Structural Parameters for 2,3-Diphosphino-1,4-diphosphonium Cations

[Me_3P-PPh-PPh-PMe_3], **4′a**

(*R,S*) meso-diastereomer favored (ΔE = 6.3 kJ/mol)

anti conformer favored

	P−P (Å)[a]	$C_{R'}$−P−P (°)[a]	$\tau_{R'}$ (°)	τ_{PR3} (°)
experimental	2.2041(9) [mid] 2.2318(12)	101.02(8)	180	180
calculated	2.259 [mid] 2.286	102.2	180.0	180.0

[Me_3P-PMe-PMe-PMe_3], **4′b**

(*R,R*)/(*S,S*)-diastereomer favored (ΔE = 15.3 kJ/mol)

eclipsed conformer favored

	P−P (Å)[a]	$C_{R'}$−P−P (°)[a]	$\tau_{R'}$ (°)	τ_{PR3} (°)
experimental	2.192(2) [mid] 2.243(2) 2.191(2)	101.1(2) 102.8(2)	31.25(11)	−126.72(3)
calculated	2.242 [mid] 2.265	107.2	−1.9	−152.3

[a] [mid] indicates the central P−P bond, while the indicated $C_{R'}$−P−P values describe the angle subtended by the central substituent (Me, Et, Ph) and this bond. $\tau_{R'}$ indicates the C−P−P−C torsion angle between the central substituents, while τ_{PR3} indicates the P−P−P−P torsion angle of the phosphorus backbone.

have less geometric flexibility than tricoordinate phosphine centers. The $^{1}J_{AB}$ coupling constants for derivatives of **4** (Table 3) are consistent with the established range of $^{1}J_{PP}$ values for phosphinophosphonium cations.[2] However, the $^{1}J_{AA'}$ values are significantly smaller (*ca.* 100 Hz) for derivatives with phenyl substituents at the phosphine centers (**4a**, **4′a**).

To assess the factors responsible for defining the conformers and diastereoselectivity that are observed in the solid state structures, comparative ground-state energy calculations were performed using B3LYP/6−31+G(d) for staggered, eclipsed and gauche conformations of the *meso*- and (*S,S*)-diastereomers for dications **4′a** and **4′b** in the gas phase. Calculated structural parameters for the lowest energy structures are presented in Table 5. In all cases, the results are in agreement with the experimental solid state structures: the *R,S meso*-isomer is favored for **4′a**, (R′ = Ph, $|\Delta E|$ = 6.3 kJ/mol) while the (*R,R*)/(*S,S*) diastereomer is favored for **4′b** (R′ = Me, $|\Delta E|$ = 15.3 kJ/mol). It is noteworthy that the energy difference between the two diastereomers of **4′a** is small, providing a rationale for observation of a mixture of diastereomers in the solution state ^{31}P NMR spectra.

The thermodynamically favored staggered conformation for the *R,S meso*-diastereomer is explained (Figure 4) in terms of the minimization of steric interactions between both the Me_3P termini and the central substituents [$\tau_{R'} = \tau_{PR3} = 180°$] in this rotamer. Indeed, computational studies that begin with an eclipsed initial geometry for the *R,S meso*-diastereomer undergo geometry optimization to give the staggered conformation. The thermodynamic preference of the (*R,R*)/(*S,S*) diastereomer for the eclipsed conformation seems counterintuitive, but it suggests that steric interactions between the terminal phosphonium substituents play a dominant role in determining the lowest energy conformer (Figure 4). Even for smaller terminal ligands (PH_3) or larger central alkyl substituents at the internal phosphine sites, computational models indicate that the eclipsed conformation of the (*S,S*) diastereomer is favored over the gauche or staggered conformers. In addition, calculations on the theoretical structure of **4′d** (R′ = ^{i}Pr) demonstrate that the (*R,R*)/(*S,S*) racemic mixture is thermodynamically favored over the *meso*-diastereomer even for more sterically hindered alkyl derivatives ($|\Delta E|$ = 19.5 kJ/mol), suggesting that the single diastereomer observed for both **4c** and **4d** in solution is the (*R,R*)/(*S,S*) racemic mixture.

The calculated structural parameters for **4′a** closely parallel those experimentally determined in the solid state (Table 5). In contrast, the calculated parameters for **4′b** more closely resemble those of the conformer for **4b** that is observed in the solid state, possessing a nearly idealized eclipsed conformation [$\tau_{R'} = 1.9°$], and a correspondingly larger P−P−P−P torsion angle [τ_{PR3} = 152.3°] and $C_{R'}$−P−P angle [107.2°]. Crystal packing effects and lattice energy in the solid state may be a significant contributor to the deviation from calculated gas-phase parameters of **4′b**.

Summary

New chlorophosphinophosphonium ions have been prepared and comprehensively characterized. Reductive coupling of these cations using Ph_3P gives the first acyclic *catena*-2,3-diphos-

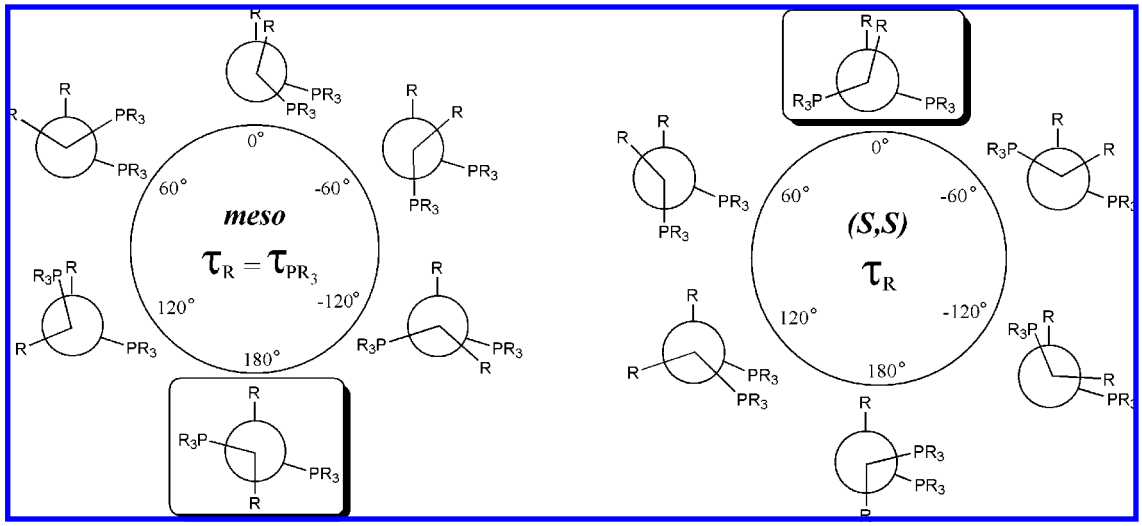

Figure 4. Representative conformations of the *meso*- and (*S,S*)-diastereomers. Idealized torsion angles between the central R-substituents are indicated (τ_R), and the preferred conformation in the gas phase is highlighted.

phino-1,4-diphosphonium ions. These new dications are also formed in a one-pot combination of a dichlorophosphine, a tertiary phosphine and Me_3SiOTf. Quantitative ligand exchange reactions are observed when derivatives of $[Ph_3P\text{-}PR'\text{-}PR'\text{-}PPh_3][OTf]_2$ react with Me_3P, demonstrating the coordinative nature of the terminal phosphine-phosphonium bonds and implicating the diphosphenium cation acceptor. The diastereoselectivity of the reactions and the conformational preferences observed in the solid state structures have been interpreted in the context of computational models.

Acknowledgment. We thank the Natural Sciences and Engineering Research Council of Canada, the Killam Foundation, the Canada Research Chairs Program, the Canada Foundation for Innovation, the Nova Scotia Research and Innovation Trust Fund, the Walter C. Sumner Foundation, and the Eliza Ritchie Scholarship for funding, Ulli Werner-Zwanziger for obtaining solid state NMR spectroscopic data, and Sarah Whittleton for invaluable discussions on computational methodology.

Supporting Information Available: Comparisons of simulated and experimental $^{31}P\{^1H\}$ NMR spectra for [**4c**][OTf]$_2$, [**4d**][OTf]$_2$, and [**4′b**][OTf]$_2$, the solid-state ^{31}P CP/MAS NMR spectrum of [**4a**][OTf]$_2$, complete ref 25, and crystallographic information files. This material is available free of charge via the Internet at http://pubs.acs.org.

JA805911A

(34) Gee, M.; Wasylishen, R. E.; Ragogna, P. J.; Burford, N.; McDonald, R. *Can. J. Chem.* **2002**, *80*, 1488–1500.
(35) Burford, N.; Cameron, T. S.; LeBlanc, D. J.; Losier, P.; Sereda, S.; Wu, G. *Organometallics* **1997**, *16*, 4712–4717.